

An Unconventional CCCH-Tandem Zinc-Finger Protein Represses Secondary Wall Synthesis and Controls Mechanical Strength in Rice

Dongmei Zhang^{1,3}, Zuopeng Xu¹, Shaoxue Cao^{1,3}, Kunling Chen², Shance Li^{1,3}, Xiangling Liu¹, Caixia Gao², Baocai Zhang^{1,*} and Yihua Zhou^{1,3,*}

¹State Key Laboratory of Plant Genomics, Institute of Genetics and Developmental Biology, Chinese Academy of Sciences, Beijing 100101, China

²State Key Laboratory of Plant Cell and Chromosome Engineering, Institute of Genetics and Developmental Biology, Chinese Academy of Sciences, Beijing, China

³University of Chinese Academy of Sciences, Beijing 100049, China

*Correspondence: Baocai Zhang (bczhang@genetics.ac.cn), Yihua Zhou (yhzhou@genetics.ac.cn)

<https://doi.org/10.1016/j.molp.2017.11.004>

ABSTRACT

Secondary walls, which represent the bulk of biomass, have a large impact on plant growth and adaptation to environments. Secondary wall synthesis is switched and regulated by a sophisticated signaling transduction network. However, there is limited understanding of these regulatory pathways. Here, we report that ILA1-interacting protein 4 (IIP4) can repress secondary wall synthesis. IIP4 is a phosphorylation substrate of an Raf-like MAPKKK, but its function is unknown. By generating *iip4* mutants and relevant transgenic plants, we found that lesions in *IIP4* enhance secondary wall formation. Gene expression and transactivation activity assays revealed that IIP4 negatively regulates the expression of *MYB61* and *CESAs* but does not bind their promoters. IIP4 interacts with *NAC29/NAC31*, the upstream regulators of secondary wall synthesis, and suppresses the downstream regulatory pathways in plants. Mutagenesis analyses showed that phosphomimic IIP4 proteins translocate from the nucleus to the cytoplasm, which releases interacting NACs and attenuates its repression function. Moreover, we revealed that IIPs are evolutionarily conserved and share unreported CCCH motifs, referred to as unconventional CCCH-tandem zinc-finger proteins. Collectively, our study provides mechanistic insights into the control of secondary wall synthesis and presents an opportunity for improving relevant agronomic traits in crops.

Key words: secondary wall synthesis, regulatory pathway, repressor, zinc finger, rice

Zhang D., Xu Z., Cao S., Chen K., Li S., Liu X., Gao C., Zhang B., and Zhou Y. (2018). An Unconventional CCCH-Tandem Zinc-Finger Protein Represses Secondary Wall Synthesis and Controls Mechanical Strength in Rice. *Mol. Plant*. **11**, 163–174.

INTRODUCTION

Secondary walls are not only characteristic plant cellular structures but also play important roles in plant growth. Three major polymers are assembled and deposited between the primary walls and plasma membranes of specialized cells to form secondary walls. Cellulose microfibrils constitute a load-bearing network and are further crosslinked to lignin and hemicellulose, such as xylan, mannan, and xyloglucan, to build a rigid yet flexible structure (Taylor-Teeples et al., 2015). Based on the physicochemical properties of this structure, secondary walls provide mechanical support for upright growth and hydrophobicity for water transportation. It is conceivable that deposition of secondary walls in plant cells is a critical event for plants in adapting to terrestrial environments (Zhong and Ye, 2014; Watanabe et al., 2015). Secondary walls represent the

bulk of the renewable plant biomass, and their economic value can extend to human health as well as industrial and energy production. Therefore, understanding how plants synthesize secondary walls is of a great significance.

Several cell types, such as tracheary elements, interfascicular fibers, the endotheicum, and trichomes, have deposited secondary walls. Although these walls include cellulose, xylan, and/or lignin, the proportion of the three components varies in different cell types, suggesting secondary wall heterogeneity (Zhong and Ye, 2007). To achieve heterogeneity, plants have evolved a sophisticated mechanism to simultaneously orchestrate multiple

genes participating in secondary wall synthesis. Based on genetic and molecular studies, a hierarchical regulatory network has been identified in *Arabidopsis* (Zhong and Ye, 2007, 2014), in which NAC transcription factors work as master switches at a higher level, while MYB transcription factors function as the lower-level master switches. Other factors, such as CCCH-type zinc-finger protein *Arabidopsis* C3H14/L and poplar C3H17/18, act downstream of the MYB transcription factors (Ko et al., 2009; Kim et al., 2012; Chai et al., 2014). The current model suggests that more than 65 transcription factors are involved in controlling secondary wall synthesis, which may directly target the cell wall synthesizing genes and/or act as switches of a cascade of several transcription factors (Handakumbura and Hazen, 2012). Most of the components in the regulatory network function redundantly and/or have cell type-specific expression profiles (Kubo et al., 2005; Mitsuda et al., 2005; Zhong et al., 2007). Single mutants usually show no phenotypes (Mitsuda and Ohme-Takagi, 2008; McCarthy et al., 2009), indicating that the regulatory network is flexible and complex. The presence of both activators and repressors in turning on/off regulatory pathways demonstrates this complexity. Compared with activators, repressors seem to be more effective at fine-tuning regulatory pathways and subtly controlling the network. However, the identified repressors that control secondary wall synthesis are very limited. WRKY12, which was characterized in *Medicago* and *Arabidopsis*, has a suppression effect on the NST2-mediated signaling pathway (Wang et al., 2010). MYB proteins can also work as transcriptional repressors. For example, MYB4 and its orthologs in different plant species negatively regulate lignin biosynthesis (Jin et al., 2000; Fornale et al., 2010; Legay et al., 2010). In addition to transcriptional regulation, protein–protein interactions can also trigger repression. Secondary wall NACs likely form dimers (Yamaguchi et al., 2008). Truncation of the activation domain of SND1 and VNDs interrupt dimer formation and suppress transcription of downstream genes (Yamaguchi et al., 2008; Li et al., 2012b; Zhao et al., 2014). VND-INTERACTING2 (VIN2) has been found to interact with VND7 and interrupt secondary wall synthesis (Yamaguchi et al., 2010). The interaction between KNAT7, a type-II KNOX protein, and OFP4 (OVATE FAMILY PROTEIN4) or MYB75, is also imperative in disturbing secondary wall synthesis (Li et al., 2011; Bhargava et al., 2013). Even so, more negative regulators remain to be discovered.

Controlling the when, where, and what of composition of secondary wall synthesis is an important issue for understanding the programming of secondary wall deposition. It is believed that various internal and external signals can trigger switches of cell wall synthesis. Brassinosteroid and light have been found to promote CESA gene transcription during hypocotyl elongation in *Arabidopsis* (Leivar and Quail, 2011; Xie et al., 2011). Gibberellin regulates secondary wall synthesis via DELLA-NAC signaling cascades (Huang et al., 2015). Kinases are critical regulators that perceive these signals and transmit them downstream by phosphorylating their targets. FEI1 and FEI2 are two leucine-rich repeat receptor-like kinases in *Arabidopsis* and can activate cell wall biosynthesis (Xu et al., 2008). Recently, a cell wall-associated kinase was reported to enhance the expression of secondary wall synthesizing genes and secondary wall formation, consequently improving resistance to bacterial diseases (Hu et al., 2017). We previously identified Increased Leaf Angle1

(ILA1), a Raf-like MAPKKK protein (Ning et al., 2011). Mutation of *ILA1* inhibits transcription of multiple cell wall synthesis genes and results in compromised secondary wall formation in rice (Ning et al., 2011). Although the impacts of these kinases on cell wall formation are obvious, the signal transduction pathways that they mediate remain elusive.

IIPs have been reported to be ILA1-interacting proteins and are phosphorylated by ILA1 (Ning et al., 2011). IIPs exist in all plant species and constitute a small family, although none of them have been characterized. Here, we present multiple lines of evidence from genetic and molecular biological analyses demonstrating that IIP4 is an uncanonical CCCH-tandem zinc-finger protein and acts as a repressor to control secondary wall synthesis. IIP4 interacts with NAC29/31, the higher-level regulators of secondary wall synthesis, and suppresses the NACs-mediated regulatory cascade as well as secondary wall synthesis in rice. The phosphorylation form of IIP4 changes the protein subcellular location and attenuates its repression effect. Our study thus reveals the IIP4 acts in signal transduction and provides a mechanism for how plants exert control on secondary wall synthesis.

RESULTS

Lesions in *IIP4* Alter Secondary Wall Thickness and Its Mechanical Strength

IIPs are a small group of proteins that were identified by yeast-two hybrid screen using ILA1 as bait (Ning et al., 2011). To determine the physiological processes in which they are involved, we knocked out *IIP4*, a highly expressed member, using the CRISPR/Cas9 genome-editing approach (Shan et al., 2013). Genotyping the resulting transgenic plants showed a single nucleotide inserted at the 603-bp position of the *IIP4* coding region, resulting in a reading frame shift and premature stop codon (Figure 1A and 1B). As the mutation causes the loss of the cleavage site of the restriction enzyme *PvuII*, a cleaved amplification polymorphism sequence-tagged site (CAPS) marker was developed for rapid genotyping (Figure 1C). We further generated a polyclonal antibody against IIP4. Western blotting with this antibody visualized one band and no signal in wild-type and mutant plants (Figure 1D), indicating the specificity of this antibody and absence of an intact translational product in the mutants.

Next, we found that *iip4* plants had slightly dwarfed but hard culms compared with wild-type (Figure 1E and 1F). Anatomic analyses showed that the sclerenchyma cell wall of *iip4* mutants became obviously thicker than that of wild-type plants (Figure 2A–2C). We also compared the cell wall composition of wild-type and *iip4* internodes. The amount of cellulose and lignin increased in *iip4* internodes (Figure 2D), whereas the xylose content was not significantly altered (Supplemental Table 1), indicating that the synthesis of xylan, a major hemicellulose of the rice cell wall, was almost unchanged in the mutant. Therefore, the increased wall thickness in *iip4* results from an increased abundance of cellulose and lignin. As cellulose and lignin are the two major components of secondary walls, IIP4 may function as a negative regulator of secondary wall formation. To confirm this hypothesis, we generated transgenic plants overexpressing *IIP4* (*IIP4*-OX) and its knockdown

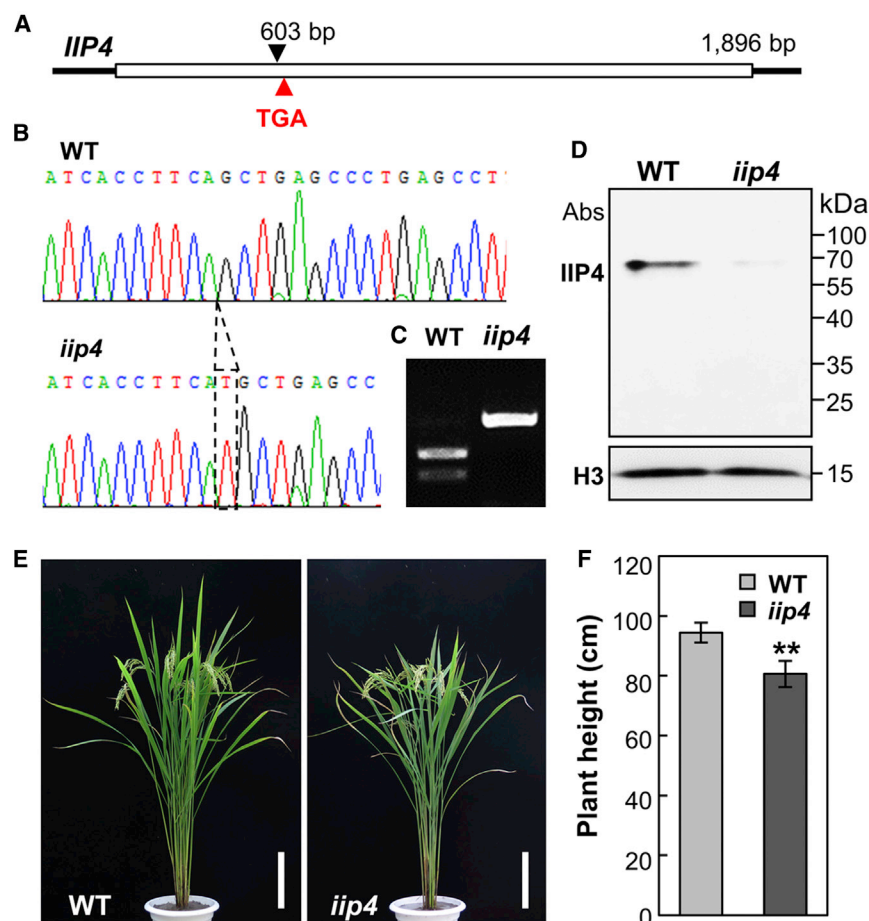


Figure 1. Generation of the *iip4* Mutant by CRISPR/Cas9.

(A) The targeting site of *IIP4*. The black arrowhead indicates the insertion site of the single base pair (T). The red arrowhead indicates the stop codon introduced by the insertion.

(B) Sequencing confirmation of the *IIP4* gene in wild-type (WT) and *iip4* plants. The inserted base pair is indicated by dashed lines.

(C) Genotyping *iip4* plants by a CAPS marker.

(D) Western blotting of IIP4 in total protein extracted from wild-type and *iip4* internodes using the anti-IIP4 antibody. The amount of protein loaded in each lane was determined by probing with the anti-histone H3 antibody. Abs, antibodies.

(E) Phenotypes of wild-type and *iip4* mature plants. The images are representative of 20 plants. Scale bars, 20 cm.

(F) Quantification of the plant height of wild-type and *iip4* plants. Error bars represent the mean \pm SD ($n = 30$). ** $P < 0.01$ according to Student's *t*-test.

expressed in the examined cells, and more transcripts were detected in cells that had secondary walls (Figure 3B).

Although two major components of secondary wall were increased in *iip4*, cellulose is the most abundant polymer; MYB61-CESAs represents an identified regulatory pathway for cellulose synthesis in rice (Huang et al., 2015). We therefore chose

plants by RNA interference (*IIP4*-Ri). *IIP4*-OX plants had a sprawling appearance, whereas knockdown plants had an erect architecture (Supplemental Figure 1A and 1B). Scanning electron microscopy (EM) revealed that *IIP4*-OX plants had a slightly thinner wall thickness and that *IIP4*-Ri plants had an increased wall thickness in sclerenchyma cells (Supplemental Figure 1C and 1D), which was in agreement with the alterations in the cellulose and lignin contents (Supplemental Figure 1E and 1F). As the altered wall thickness in sclerenchyma cells may affect the mechanical strength, we examined the breaking force of the internodes of these rice plants. As opposed to *IIP4*-OX plants, which showed a reduced breaking force, *iip4* mutant and knockdown plants exhibited increased mechanical strength (Figure 2E and Supplemental Figure 1G). Therefore, *IIP4* is important for secondary wall formation in rice plants.

IIP4 Acts as a Negative Regulator

To understand how *IIP4* affects secondary wall thickening, we investigated the expression profile of this gene in rice plants. Online microarray data showed that *IIP4* is ubiquitously expressed with more transcripts in the internodes (Supplemental Figure 2A). To explore the expression of *IIP4* at cellular level, we harvested secondary wall-rich sclerenchyma cells and vascular bundles and primary wall-rich parenchyma cells from young internodes by laser microdissection (Figure 3A). qPCR performed in these cells revealed that *IIP4* was

this pathway as a representative to investigate the underlying mechanism by which *IIP4* modulates secondary wall synthesis. We first compared the expression of three cellulose synthase (*CESA*) genes by qPCR. More transcripts were detected in sclerenchyma cells of *iip4* plants (Figure 3C and Supplemental Figure 2B). Moreover, *MYB61*, the upstream regulator of *CESAs*, showed increased expression in both sclerenchyma and parenchyma cells (Figure 3D). These findings suggest that *IIP4* coordinates cellulose synthesis by regulating the *MYB61*-*CESAs* pathway. Next, we explored the transactivation activity of *IIP4* in *Arabidopsis* protoplast cells. The reduced activity in cells that expressed either *IIP4* or *IIP4*-SRDX containing a dominant repressive motif (Hiratsu et al., 2003) indicated that *IIP4* has suppressive activity (Supplemental Figure 2C). To validate this activity on the *MYB61*-*CESAs* regulatory pathway, we co-expressed *IIP4*, which was driven by CaMV 35S promoter, and the luciferase reporter, which was driven by *MYB61* or *CESA* promoter in *Arabidopsis* protoplasts. Expression of *MYB61* and *CESAs* was downregulated by *IIP4*, as indicated by the reduced luciferase activities (Figure 3E). These results suggest that *IIP4* negatively regulates the *MYB61*-*CESAs* pathway.

IIP4 Interacts with the Secondary Wall Regulators *NAC29* and *NAC31*

We then examined whether *IIP4* can directly bind to the promoters of *MYB61* and/or *CESAs*. Chromatin immunoprecipitation

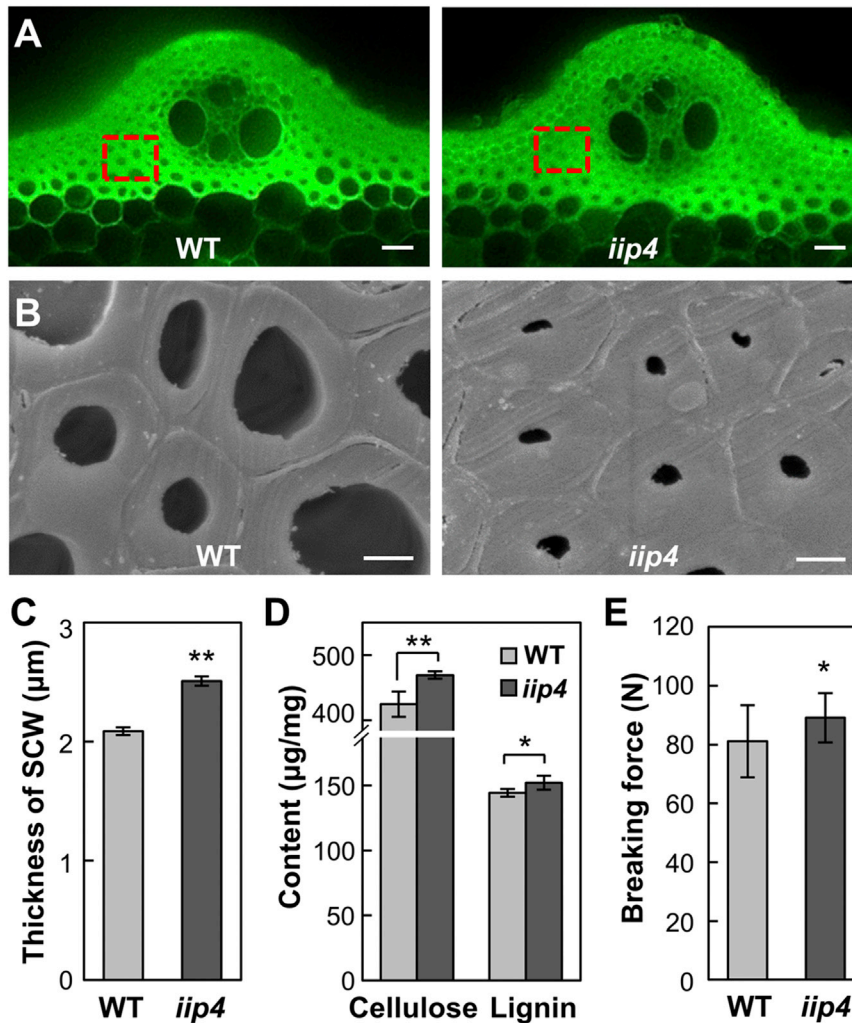


Figure 2. IIP4 Affects Secondary Wall Formation.

(A) Hand-cut cross sections of wild-type (WT) and *iip4* internodes. The red dashed lines circle the locations observed by scanning EM. Scale bars, 20 μm.

(B) Scanning EM images to show cortex sclerenchyma cells in wild-type and *iip4* internodes. Scale bars, 2 μm.

(C) Quantification of the thickness of the secondary cell wall. Error bars represent the mean ± SE ($n = 100$).

(D) The cellulose and lignin contents in the internodes of wild-type and *iip4* plants. Error bars represent the mean ± SD of three replicates.

(E) Measurement of the breaking force of wild-type and *iip4* internodes. Error bars represent the mean ± SD ($n = 20$).

* $P < 0.05$, ** $P < 0.01$ according to Student's *t*-test.

(ChIP) assays were performed in wild-type plants using the IIP4 antibody. None of the promoter fragments were enriched, although the examinations covered the full 2200-bp promoter region of *MYB61* as well as the promoter regions of the *CESAs* that contained key motifs (Supplemental Figure 3), in accordance with the fact that IIP4 does not possess a DNA binding domain as predicted by sequencing alignment (Ning et al., 2011).

We therefore assumed that IIP4 might function via a protein–protein interaction. Split-luciferase complementation assays did not reveal interactions between IIP4 and *MYB61* or *CESAs* (Supplemental Figure 4A), but revealed interaction between IIP4 and *NAC29* or *NAC31* (Figure 4A and Supplemental Figure 4B), the two upstream direct regulators of *MYB61* (Huang et al., 2015). The interaction was further confirmed by co-immunoprecipitation (Co-IP) analysis in transgenic rice plants that expressed GFP-tagged *NAC29* or *NAC31* (Figure 4B and Supplemental Figure 4C). Co-IP assays performed in transgenic plants expressing BC3-GFP (Xiong et al., 2010) were regarded as negative controls. Bimolecular fluorescence complementation (BiFC) assays further verified that the interaction occurred in the nuclei (Figure 4C). To determine the effect of the interaction *in vivo*, we conducted a transactivation activity assay in *Arabidopsis* protoplasts. Luciferase activity

promoted by expressing *NAC29* was significantly suppressed by co-expression of *IIP4* (Figure 4D). These results indicate that IIP4 repressed the *MYB61*-*CESAs* regulatory pathway by interacting with *NAC* transcriptional factors.

IIP4 Functions in Developing Internodes

Rice internode development involves secondary wall synthesis initiation, accumulation, and termination. It has been shown that the *MYB61*-*CESAs* regulatory pathway is activated at the early stages of internode development and is gradually attenuated during maturation (Huang et al., 2015). To

validate the IIP4 function in this natural physiological process, we divided the developing internodes into eight sections (S1–S8) from the bottom up. By performing qPCR analysis on each section, *IIP4* was found to be upregulated from section 1 to section 4, peaked at section 4, then decreased and stayed at a relatively high level until the internodes became mature (Figure 5A). Western blotting revealed significant IIP4 signals from section 3 to section 7 (Figure 5B), suggesting that IIP4 is involved in internode development. To determine in which development stage IIP4 participates, we compared the expression of three secondary wall *CESAs* in developing internodes of wild-type and *iip4* plants. Consistent with the increased cellulose content (Figure 2D), the mutant internodes showed more *CESA* transcripts at later development stages (Figure 5C–5E). Therefore, IIP4 is likely involved in the process of “turn-off” of secondary wall formation, such as shutting down the *MYB61*-*CESAs* pathway, when internodes enter maturation.

Phosphorylation of IIP4 Attenuates its Suppression Effect on the *MYB61*-*CESAs* Regulatory Pathway

Previous work has demonstrated that IIP4 is a phosphorylated substrate of *ILA1* (Ning et al., 2011). To investigate phosphorylated residues of IIP4, we performed *in vitro*

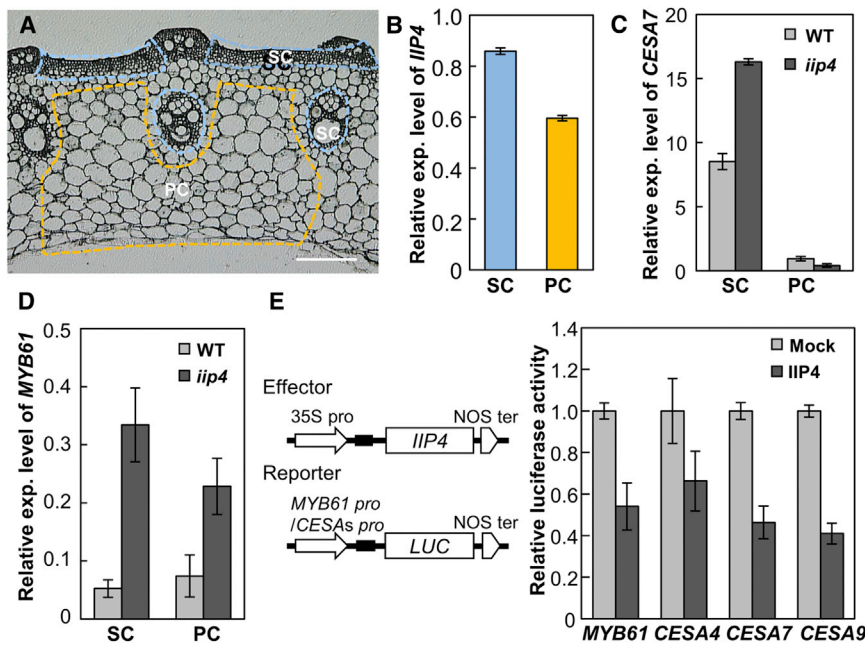


Figure 3. IIP4 Negatively Regulates the MYB61-CESAs Regulatory Pathway.

(A) A cross-section of young rice internodes. The colored dashed lines indicate the cell types harvested by laser microdissection. SC, sclerenchyma cells and vascular bundles; PC, parenchyma cells. Scale bar, 100 μ m.

(B) qPCR analysis of cells harvested in (A) to show the relative expression level of *IIP4* to rice *HNR*. Error bars represent the mean \pm SD of three replicates.

(C and D) qPCR analysis of sclerenchyma cells (SC) and parenchyma cells (PC) harvested from wild-type (WT) and *iip4* internodes to show the relative expression level of *CESA7* and *MYB61* compared with rice *TP1* and *HNR*, respectively. Error bars represent the mean \pm SD of three replicates.

(E) Transcription activation assays performed by transfecting protoplasts with the constructs shown in the left panel. Error bars represent the mean \pm SD of three replicates.

phosphorylation analysis. As shown in Supplemental Figure 5, three phosphorylation sites (S275, S584, and T594) were repeatedly detected. Phosphorylation can change protein localization, protein conformation, and activity. To determine the effects of phosphorylation, we mutated the three amino acids into alanine (IIP4^{3A}) or aspartic acid (IIP4^{3D}) to mimic the unphosphorylated and phosphorylated status of IIP4, respectively. By transfecting rice protoplasts with constructs that contain IIP4, IIP4^{3A}, or IIP4^{3D} fused to GFP, the major IIP4 and IIP4^{3A} signals were found to be localized in the nucleus, whereas those of IIP4^{3D} were mainly detected in the cytoplasm (Figure 6A–6F). As IIP4-NAC29 interaction occurs in the nucleus (Figure 4C), it was hypothesized that the altered protein location may alter the suppression activity of IIP4 on the MYB61-CESAs regulatory pathway. We therefore explored the transactivation activity in cells that co-expressed NAC29 and the mutated versions of IIP4. As shown in Figure 6G, luciferase activity that was induced by NAC29 was significantly suppressed by expressing wild-type or non-phosphomimic IIP4, but was not affected by expressing phosphomimic IIP4.

To obtain further proofs from plants, we investigated the IIP4 phosphorylation status in wild-type and *ila1* mutants. Because phosphorylation alters IIP4 localization, we compared the location pattern of IIP4 by fractionation of the total proteins extracted from wild-type and *ila1* plants into nuclear and cytoplasmic fractions and probed them with anti-IIP4 antibody. In *ila1* plants, more IIP4 proteins were found in the nuclear fraction than in wild-type plants (Figure 6H). We also detected very faint signals in the cytoplasm (Figure 6H), probably because the cytoplasmic version of IIP4 is unstable. This result suggests that more unphosphorylated IIP4 is present in *ila1* plants. Moreover, the wall thickness of sclerenchyma cells in the internodes of wild-type and *ila1* plants were analyzed by scanning EM. As expected, *ila1* led to reduced wall thickness in sclerenchyma cells (Figure 6I and 6J), in accordance with the decreased cellulose and lignin contents in *ila1* plants (Figure 6K). The xylose content

was also slightly decreased (Supplemental Table 1). Taken together, these results suggest that phosphorylation of IIP4 alters protein localization, which alleviates its suppressive effect on secondary wall synthesis.

IIP4 Is an Unconventional CCCH-Tandem Zinc-Finger Protein and Belongs to a Conserved Plant Family

Rice contains at least six IIP proteins (Ning et al., 2011). To determine whether IIPs exist in other species, we performed a comparative genomics analysis using the PLAZA 2.5 database. IIP homologs have been found in most sequenced plant species, including the moss *Physcomitrella patens* and marine algae *Micromonas*, although the member number varies (Supplemental Figure 6), implying that IIP genes likely evolved from ancient genes and their function may be fundamental for plants. To investigate the correlation between function and protein structure, we analyzed 10 representative IIP homologs from five plant species. Protein alignment showed that the central regions of these homologs are highly conserved (Supplemental Figure 7). In the conserved region, we found that cysteine (C) residues are present in a regular manner, tandem repeats of C-X₄-C-X₁₀-C-X₂-H (Figure 7A and Supplemental Figure 7), which are reminiscent of the repeats (C-X_[7,8]-C-X₅-C-X₃-H) found in the classic CCCH zinc-finger proteins. As the number and order of the C and histidine (H) residues in IIP homologs are different from those in conservative CCCH zinc-finger members (Jan et al., 2013), IIP homologs were referred to as unconventional CCCH proteins.

To determine the evolutionary relationship of IIPs, we generated a phylogenetic tree of IIP homologs from *Oryza sativa* (Os), *Sorghum bilcolor* (Sb), *Arabidopsis thaliana* (At), *Populus trichocarpa* (Pt), *Physcomitrella patens* (Pp), and *Micromonas* (MRCC), which represent dicots, monocots, woody plants, moss, and algae, respectively. The IIP members from these species were divided into two clades before the monocot/dicot divergence, in which

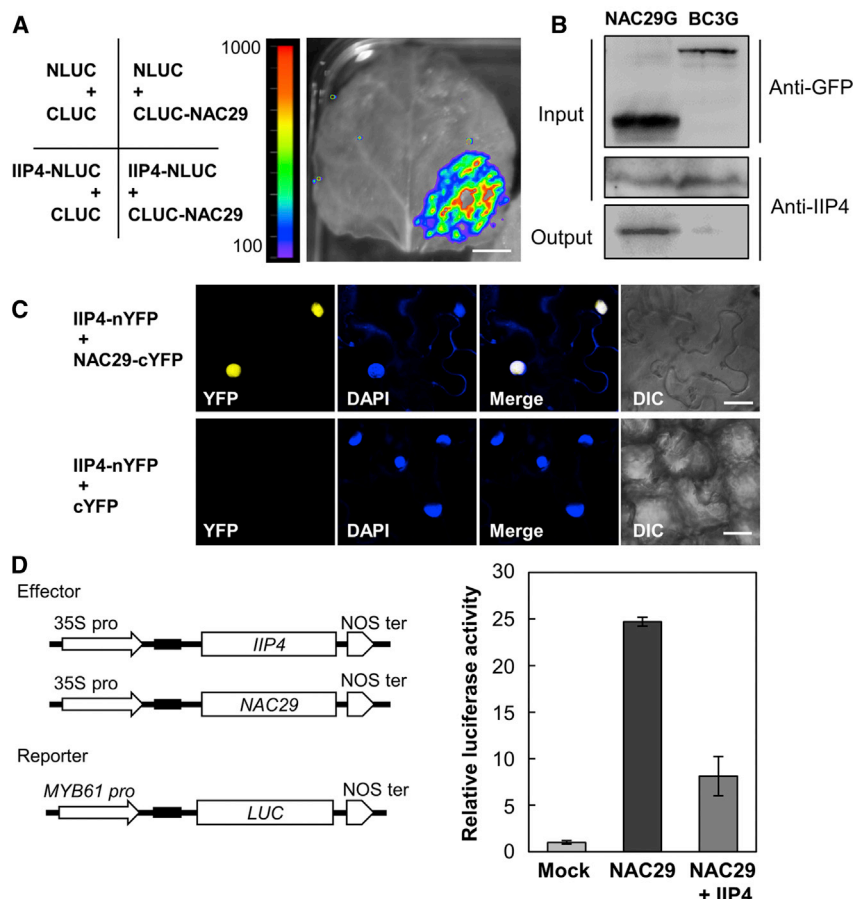


Figure 4. IIP4 Interacts with Secondary Wall Regulator NAC29.

(A) Split-luciferase complementation assay, showing the interaction between IIP4 and NAC29 in *N. benthamiana* leaves infiltrated with the construct combinations shown in the left panels. Scale bar, 1 cm.

(B) Co-immunoprecipitation of IIP4 and NAC29 in transgenic plants overexpressing GFP-NAC29. The protein sample extracted from the transgenic plants overexpressing BC3-GFP was used as a negative control.

(C) BiFC analysis of the interaction between IIP4 and NAC29. Infiltrations with the empty vector were used as negative controls. DAPI was used to visualize nuclei. Merge, merged images of YFP and DAPI. Scale bars, 20 μ m.

(D) Transcription activation assays by transfecting protoplasts with the constructs (shown in the left panel), showing that IIP4 repressed luciferase activity in cells co-expressing NAC29. Error bars represent the mean \pm SD of three replicates.

To facilitate the co-regulation of numerous synthesizing genes, this network is likely subtly adjusted by many activators and repressors. However, very few repressors have been identified.

IIP4, which has been identified as an ILA1-interacting protein, has an uncharacterized function. Here, we used the CRISPR/Cas9 genome-editing approach to generate a

mutant in which translation of IIP4 is prematurely terminated. Probing with the anti-IIP4 antibody revealed that no IIP4 proteins were detected in mutants. *iip4* can be considered to be a null mutant. Anatomical and compositional analyses showed that the *iip4* mutant has an increased secondary wall thickness and more cellulose and lignin abundance. Therefore, IIP4 may act as a repressor of secondary wall formation. This conclusion was corroborated by the phenotypes of *IIP4* overexpression and knockdown plants, which showed reciprocal tendency on the cellulose and lignin contents. Further molecular proof came from qPCR analysis, which revealed that expression of *MYB61* and *CESAs* was upregulated in *iip4* plants, and from transactivation activity assays, which showed that IIP4 repressed transcriptions promoted by the *Gal4*, *MYB61*, and *CESAs* promoters. Based on these findings, we concluded that IIP4 is an unreported repressor of secondary wall synthesis.

IIP4 Functions in the Upstream of the MYB-CESAs Regulatory Network

However, IIP4 failed to bind the promoter regions of *MYB61* and *CESAs*, as revealed by ChIP-PCR analysis, indicating that IIP4 cannot function as a traditional transcriptional factor. Its repression effect is mediated by a protein-protein interaction, like KNAT7, a well-known repressor of secondary wall synthesis (Li et al., 2012a). KNAT7 has been reported to negatively regulate secondary wall thickness by interacting with MYB75 or OFP4 (Zhong et al., 2008; Li et al., 2011, 2012a; Bhargava et al.,

those from *P. patens* were clustered together with IIP4 (Figure 7B). Grouping algae IIPs into an independent clade suggested that their function might be different from those of plants. Moreover, the IIP members were expanded in Poaceae (Figure 7B), which was probably driven by environmental adaptation. Therefore, IIP proteins belong to an ancient family and share uncanonical CCCH motifs.

DISCUSSION

IIP4 Functions as a Negative Regulator for Secondary Wall Formation

Based on progress made in the last decade, it has been shown that secondary wall biosynthesis is regulated by a hierarchy regulatory network. NAC transcription factors, such as *NST1/2*, *SND1*, and *VND6/7*, often act as master switches to turn on downstream regulatory cascades (Zhong and Ye, 2007, 2014). Tens of R2R3-MYB transcription factors, such as *MYB83*, *MYB46*, and *MYB103*, represent a second set of switches that control secondary wall formation (Dubos et al., 2010). In addition to the two types of transcription factors, homeobox HD-ZIP class III (such as PHB), CCCH-type zinc-finger proteins (such as C3H17), and WRKY transcription factors (such as WRKY12) are also involved in controlling secondary wall synthesis (Carlsbecker et al., 2010; Wang et al., 2010; Chai et al., 2014). These proteins either target cell wall synthesizing genes directly or act as switches to turn on/off regulatory cascades, resulting in a sophisticated network (Handakumbura and Hazen, 2012).

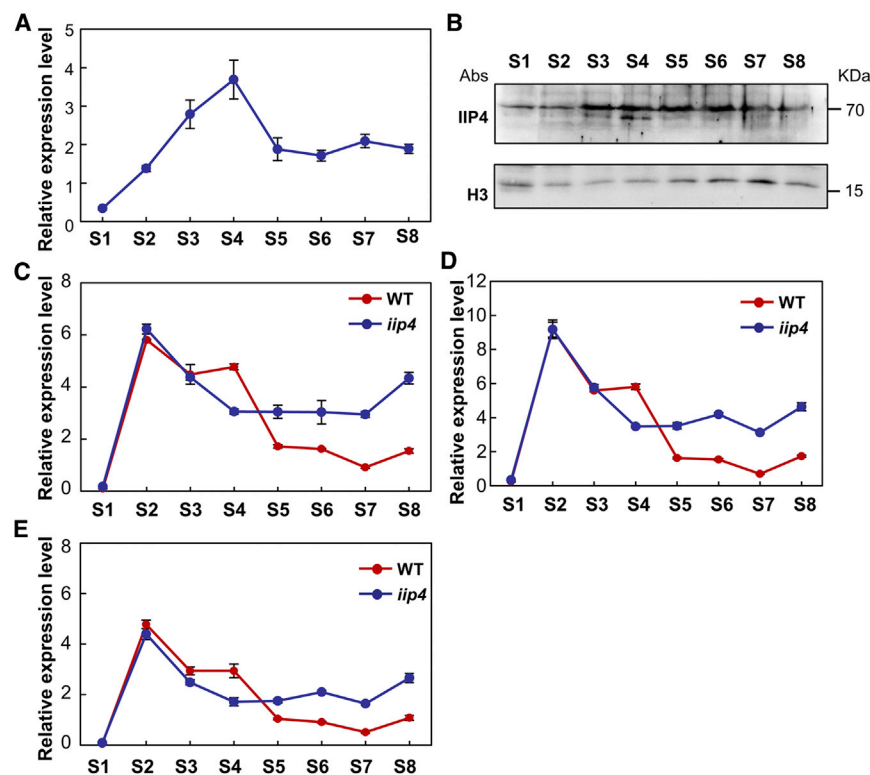


Figure 5. IIP4 Is Involved in the Internode Development Process.

(A) qPCR analysis in developing internodes that were divided into eight sections to show the relative expression level of *IIP4* to rice *HNR*. Error bars represent the mean \pm SD of three replicates. (B) Western blotting of IIP4 in dissected developing internodes using anti-IIP4 antibodies. Anti-histone H3 antibody was used to monitor the loading amount in this assay. Abs, antibodies. (C–E) qPCR analysis in dissected developing internodes of wild-type (WT) and *iip4* plants to show the relative expression level of *CESA4* (C), *CESA7* (D), and *CESA9* (E) to rice *TP1*. Error bars represent the mean \pm SD of three replicates.

ondary wall thickness as well as the cellulose and lignin contents in *ila1*. Hence, IIP4 acts as a crucial regulator by passing upstream signals to downstream regulatory pathways. As IIP4 is ubiquitously expressed, its function may extend to pathways beyond secondary wall formation.

We thus proposed a potential working model for IIP4 as summarized in Figure 8. In this model, IIP4 interacts with NAC29/31

in the nucleus to block the NACs-MYB61 regulatory pathway, probably in a dose-dependent manner. Some developmental or environmental cues may trigger ILA1 proteins target to IIP4 and phosphorylate it. Phosphorylated IIP4 proteins translocate to the cytoplasm, releasing bound NACs and promoting transduction pathways. In this study, we revealed the ILA1-IIP4 regulatory cascade and provided a mechanism for how plants fine-tune the secondary wall synthesis program.

IIPs Possess Unconventional CCCH-Tandem Motifs and Are Evolutionarily Conserved in Plants

Typical CCCH zinc-finger proteins constitute a superfamily and are important for various developmental and physiological processes by functioning in transcriptional regulation, RNA metabolism, and protein–protein interactions (Li and Thomas, 1998; Ciftci-Yilmaz and Mittler, 2008; Jan et al., 2013). Due to its functional importance, the motif structure is often used to classify zinc-finger proteins (Schumann et al., 2007). Our study revealed a previously undescribed CCCH motif structure in IIP homologs, indicating that IIPs are unconventional CCCH-tandem proteins. Based on the number and spacer sequences between the zinc fingers, the conserved C-X₄-C-X₁₀-C-X₂-H structure was found in IIP homologs of higher plants (Supplemental Table 2), inferring its fundamental role in these species. Our study showed that IIP4 regulates secondary wall synthesis. It is well known that the evolution of secondary walls conferred water-conducting and upright growth abilities of plants, which are important for plants in colonizing the terrestrial environment. Hence, critical proteins required for secondary wall synthesis emerged and evolved in early land plants. For example, NACs homologous to VND/SND/NST have arisen in the vascular ancestor moss *P. patens* (Xu et al., 2014). Here,

2013). Here, we found that IIP4 interacts with NAC29 and NAC31, the upstream regulators of the MYB61-CESAs cascade, as revealed by split-luciferase complementation and CoIP assays. BiFC analyses showed that the interaction occurs in the nucleus, and consequently suppresses the transcription activity enhanced by NAC29 in plant cells. This conclusion was corroborated in developing internodes, which involves activation of the regulatory cascades, e.g., the MYB61-CESAs pathway, during the early development stage and gradual downregulation of them during maturation (Huang et al., 2015). Increased expression of CESAs in maturing *iip4* internodes suggest that IIP4 functions in the shutdown process of secondary wall formation.

Secondary wall synthesis is spatiotemporally controlled. In response to various internal and external signals, secondary wall synthesis should be switched on at the right place and right time. Kinases are important components in responding to these signals and transmit them to regulatory cascades via phosphorylating interacting proteins. Although several kinases have been proposed to be involved in the regulation of cell wall synthesis, very few signal transduction pathways have been described for this process (Brutus et al., 2010). ILA1 is a Raf-like MAPKKK that is responsible for secondary wall formation in rice (Ning et al., 2011). However, the regulatory cascade mediated by ILA1 has not yet been characterized. IIP4 is an ILA1 phosphorylation substrate (Ning et al., 2011). In this study, we found that IIP4 blocks the NAC29-MYB61 regulatory cascade by interacting with NAC29/31. Mimicking the ILA1-mediated phosphorylated version of IIP4 changed its subcellular location to the cytoplasm and attenuated its repressive action on NAC29-driven MYB61 expression in protoplast cells. Moreover, *ila1* likely reduced phosphorylation of IIP4 as more IIP4 proteins were arrested in the nuclei, in agreement with the decreased sec-

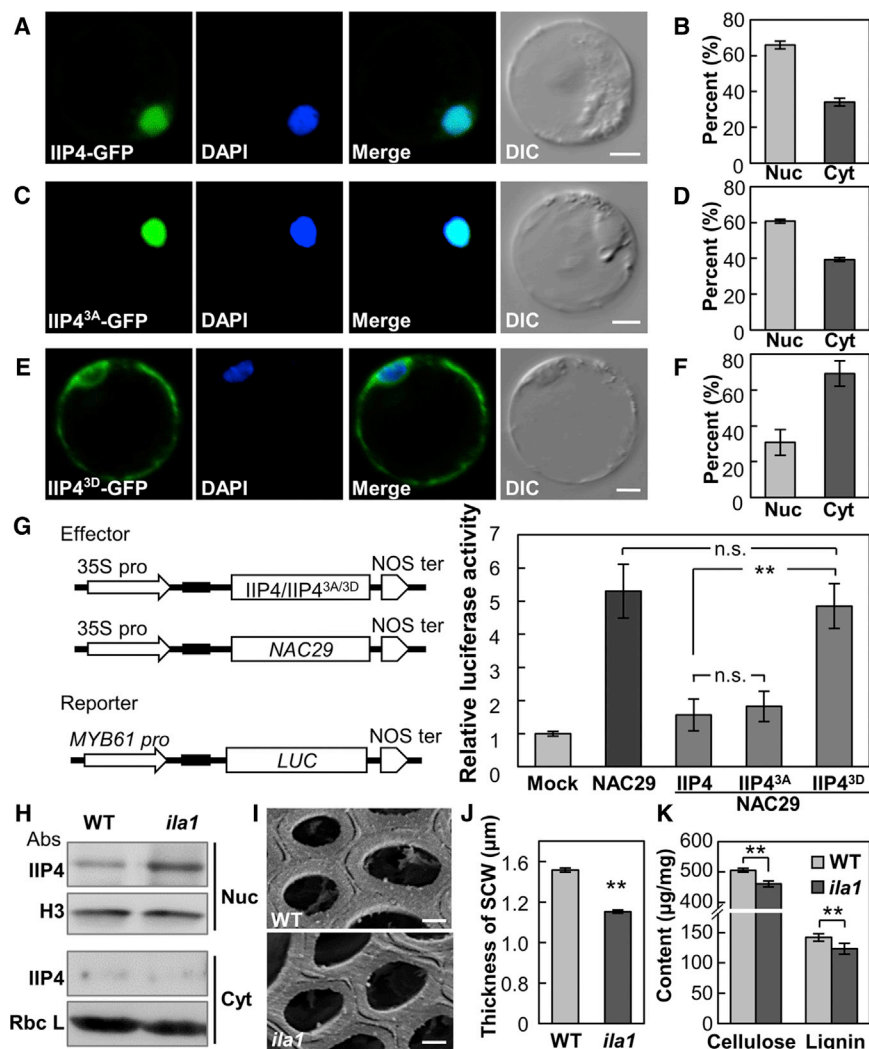


Figure 6. The Phosphorylated IIP4 Is Localized in the Cytoplasm and Relieves IIP4 Action.

(A–F) Transfecting rice protoplast cells with GFP fused to wild-type IIP4, non-phosphomimic IIP4^{S275A S584A T594A} (IIP4^{3A}), or phosphomimic IIP4^{S275D S584D T594D} (IIP4^{3D}), respectively. Quantification of cells that contained nuclear (Nuc) or cytoplasmic (Cyt) localized GFP signals. Error bars represent the mean \pm SD ($n = 200$). Scale bars, 5 μ m.

(G) Transcription activation assays by transfecting protoplasts with the constructs (shown in the left panel), showing that phosphomimic IIP4 failed to repress luciferase activity in cells expressing NAC29. Error bars represent the mean \pm SD of at least three replicates.

(H) Western blotting of IIP4 in nuclear (Nuc) and cytoplasmic (Cyt) protein fractions extracted from wild-type (WT) and *ila1* plants. Anti-histone H3 and anti-Rbc L antibodies were used to monitor the loading amount of nuclear and cytoplasmic fractions, respectively. Abs, antibodies.

(I) Scanning EM graphs of sclerenchyma cells in wild-type and *ila1* internodes. Scale bars, 2 μ m.

(J) Measurement of the sclerenchyma cell wall thickness in wild-type and *ila1* internodes. Error bars represent mean \pm SE ($n = 100$). SCW, secondary cell wall.

(K) The cellulose and lignin contents in the internodes of wild-type and *ila1* plants. Error bars represent the mean \pm SD of three replicates.

** $P < 0.01$ according to Student's *t*-test.

two IIP homologs clustered together with IIP4 were found in the moss genome. IIP4 homologs are widely found in most plant species. Together, these results imply that their fundamental function is likely related to secondary wall synthesis. Clarifying the function of IIP4 is important in elucidating the roles of other IIP homologs.

Reinforcing the secondary wall structure can improve multiple agronomic traits, such as lodging resistance, disease resistance, and grain yield (Gao et al., 2017; Hu et al., 2017; Zhang et al., 2017). We showed that lesion in IIP4 strengthened mechanical properties by activating secondary wall synthesis and enhancing secondary wall thickening. Therefore, our study sheds light on the mechanisms of secondary wall synthesis regulation and will help in the manipulation of pertinent agronomic traits in crops.

METHODS

Plant Materials and Growth Conditions

Rice plants (*O. sativa* L.), including the wild-type plants, *iip4*, *ila1*, and the relevant transgenic plants used in this study, were planted in natural seasons in the experimental fields at the Institute of Genetics and Develop-

mental Biology in Beijing (China) and in Sanya (Hainan Province, China). Etiolated rice seedlings for generating protoplast cells were grown in a dark growth chamber at 28°C. *Nicotiana benthamiana* and *A. thaliana* plants were grown in a greenhouse at 23°C under a 16-h/8-h day/night cycle.

Generation of the Transgenic Rice Plants and IIP4 Antibody

To generate *iip4* mutant, we cloned a target sequence (597–619 bp) abutting a protospacer adjacent motif into SnRNA U3 and inserted it into the vector containing a CaMV 35S driven Cas9. For generating IIP4-overexpressing plants, the full-length coding sequence (CDS) of IIP4 was amplified using the primers listed in Supplemental Table 3 and inserted into the pCambia 1300 vector between the maize *Actin* promoter and the nopaline synthase terminator. For generating IIP4 RNA interfering plants, a target sequence (736–1085 bp) was forward and inversely inserted into the pCambia 1300 vector between rice ubiquitin promoter and nopaline synthase terminator. All the resulting constructs were transfected into *Agrobacterium tumefaciens* strain EHA105 and introduced into wild-type variety Nipponbare or Zhonghua11. The anti-IIP4 polyclonal antibodies were produced in rabbits against a polypeptide of 77–180 amino acids.

Microscopy

For fluorescent microscope analyses, internodes from the development-matched wild-type and *iip4* plants were subject to freehand-cut sectioning. The sections were mounted in water containing 20% glycerol and directly observed under a microscope (Imager D2, Zeiss) with 488 nm excitation.

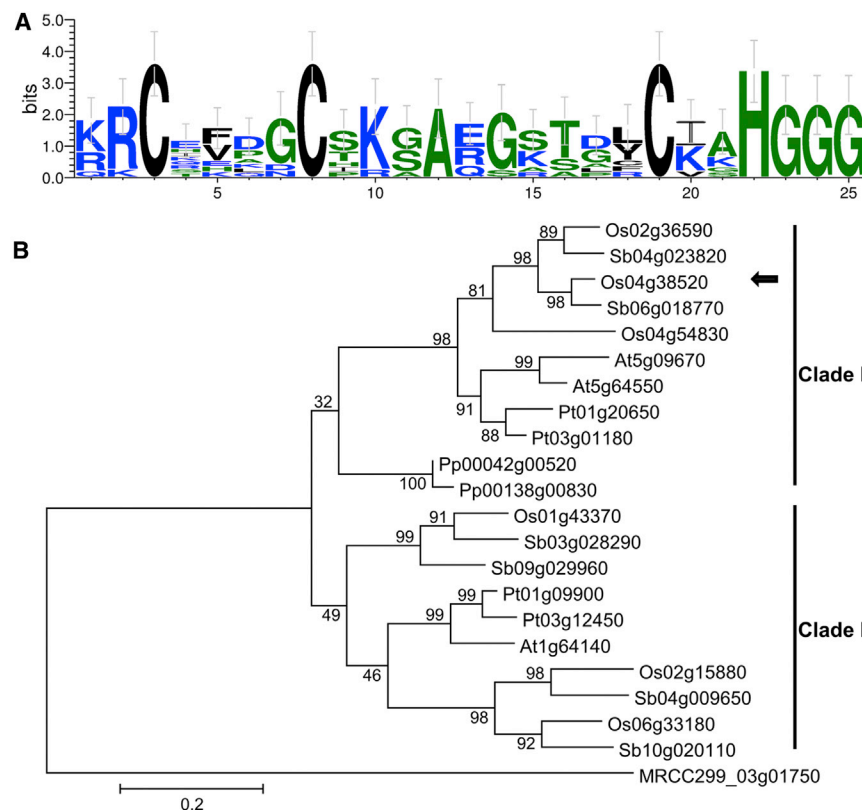


Figure 7. Sequence Analysis of IIP4 and IIP Homologs.

(A) The CCCH motif structure conserved in the IIP4 and IIP homologs.

(B) Phylogenetic trees of IIPs in *Micromonas* (MRCC), *Physcomitrella patens* (Pp), *Oryza sativa* (Os), *Sorghum bilcolor* (Sb), *Arabidopsis thaliana* (At), and *Populus trichocarpa* (Pt). The trees were constructed under the maximum-likelihood principle using MEGA 6 with bootstrap support (1000 replicates). The black arrow indicates the IIP4 protein.

collected samples with the RNeasy micro kit (Qiagen) and subjected to qPCR analyses using the primers listed in Supplemental Table 3. The ChIP analysis was performed with young internodes of wild-type plants as described by Huang et al. (2015). About 40 μ l of protein A agarose/sheared salmon sperm DNA (Millipore) that were conjugated with affinity chromatography-purified IIP4 antibodies were used for immunoprecipitation. ChIP products were analyzed by qPCR (Supplemental Table 3). Enrichment was calculated as ratio of the detected fragments to *ACTIN1* promoter.

Transactivation Analysis

The CDSs of *IIP4* and *NAC29* and promoters of *MYB61* and three secondary wall *CESA* genes were amplified (Supplemental Table 3) and cloned into the effector and reporter vectors, respectively. The resulting effector and reporter constructs were pairwise co-transfected protoplasts prepared with 4-week-old *Arabidopsis* rosette leaves. The *Renilla* luciferase gene driven by the CaMV 35S promoter was included in each assay to monitor transfection efficiency. Luciferase activities were measured with a dual-luciferase reporter assay system (Promega).

Protein Extraction and Western Blotting Assays

Total proteins were extracted from rice internodes in the buffer (25 mM Tris-HCl [pH 7.5], 2 mM EDTA, 2 mM DTT, 15 mM β -mercaptoethanol, 0.25 M sucrose, 10% glycerol, and protease inhibitor cocktail). To obtain the cytoplasmic and nuclear fractions, we ground young internodes into fine powder and lysed them with a buffer (20 mM Tris-HCl [pH 7.0], 250 mM sucrose, 25% glycerol, 20 mM KCl, 2 mM EDTA, 2.5 mM $MgCl_2$, 30 mM β -mercaptoethanol, 0.7% Triton X-100, protease inhibitor cocktail, and phosSTOP phosphatase inhibitor). The lysate was filtered with Miracloth (Calbiochem) and fractionated by centrifugation at 12 000 g. The supernatant was used as the cytoplasmic fraction. The pellet was further washed with the suspension buffer (20 mM Tris-HCl [pH 7.0], 25% glycerol, 2.5 mM $MgCl_2$, and 30 mM β -mercaptoethanol) and resuspended to be the nuclear fraction. Protein samples were separated with 12% SDS-PAGE gels, transferred to a nitrocellulose membrane, and probed with anti-IIP4 antibody (1:1000 dilution). These experiments were performed at least three times.

Protein Interactions

For split-luciferase complementation assay, the CDSs of *IIP4* and the indicated genes were cloned and fused with the N and C terminus of luciferase, respectively. The resulting constructs were transfected into *A. tumefaciens* strain C58 and pairwise co-infiltrated into the leaves of 4-week-old *N. benthamiana*. Interaction was determined based on the bioluminescence signal intensity acquired by IndiGO software. For CoIP analysis, the total proteins were extracted from internodes as described

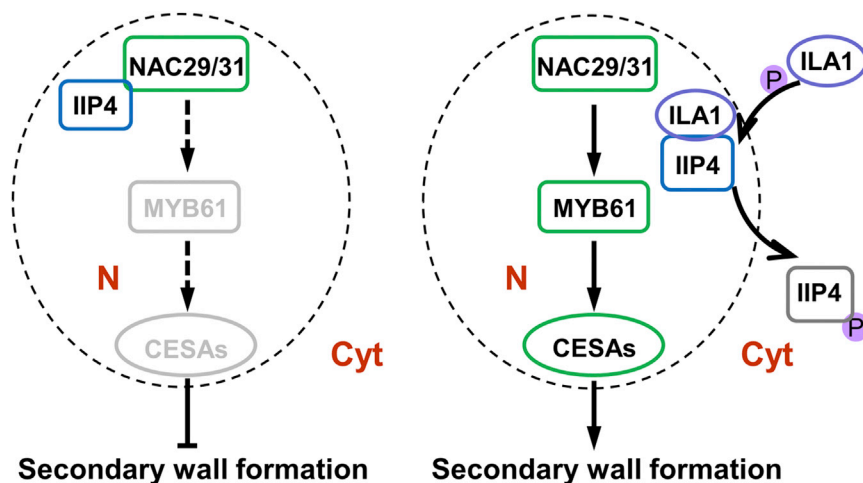
For scanning EM analysis, internodes from development-matched wild-type, *iip4*, *ila1*, and relevant transgenic plants were sliced with Gillette razor blades. The samples were then fixed in 4% paraformaldehyde (Sigma). After dehydration through a gradient of ethanol and critical point drying, the samples were sprayed with gold particles and observed with a scanning electron microscope (S-3000N; Hitachi, Tokyo, Japan). For subcellular localization assays, the CDS of *IIP4* or its mutated version were cloned and fused with GFP into pUC18 vector (Supplemental Table 3). The resulting constructs were used for transfecting rice protoplasts as described previously (Ning et al., 2011). Fluorescence signals were recorded with a confocal laser scanning microscope (Axio imager Z2, Zeiss).

Cell Wall Composition Analysis

The mature second internodes collected from wild-type, *iip4*, *ila1*, and transgenic plants were dried and ball milled into fine powders. Destarched alcohol-insoluble residues were prepared and hydrolyzed by 2 M trifluoroacetic acid. The residues were then treated in Updegraff reagent (Updegraff, 1969). The remaining pellets were treated with 72% sulfuric acid, and further subjected to analysis of the cellulose content by the anthrone method (Updegraff, 1969). The monosaccharide composition was determined by gas chromatography-mass spectrometry (Agilent) as described previously (Xiong et al., 2010). The lignin content was measured using the acetyl bromide method (Huang et al., 2015).

Gene Expression and ChIP-qPCR Assays

To examine the expression level of *IIP4* in transgenic plants, we collected development-matched internodes and subjected them to total RNA isolation. qPCR was performed with the primers shown in Supplemental Table 3. To investigate *IIP4* expression at cellular level, we embedded young internodes in paraffin and employed them for laser microdissection (Huang et al., 2015). In brief, the 12- μ m-thick sections were prepared and used for harvesting the epidermal sclerenchyma cells and parenchyma cells by the LMD 7000 laser microdissection system (Leica). Total RNA was then isolated from the

**Figure 8. The Working Model of IIP4.**

IIP4 interacts with the secondary wall regulators, such as NAC29 or NAC31, which block the NACs-MYB61 regulatory pathway. When plants perceive a certain signal, ILA1 proteins interact with IIP4 in the nucleus and phosphorylate IIP4. Phosphorylated IIP4 proteins are translocated to the cytoplasm, which releases bound NACs. The NACs-MYB61 regulatory pathway is thus turned on to synthesize secondary walls. N, nucleus; Cyt, cytoplasm; P, phosphate groups.

above and incubated with anti-GFP agarose beads (Pierce) for 3 h. The eluted samples were separated on SDS-PAGE and probed with anti-IIP4 and anti-GFP primary antibodies, respectively. For the BiFC analysis, the cDNA of *IIP4* and *NAC29* was cloned into pSPY vectors containing either amino- or carboxyl-terminal enhanced yellow fluorescence protein (EYFP) fragments. The resulting constructs were introduced into *A. tumefaciens* strain C58 and co-infiltrated into the leaves of 4-week-old *N. benthamiana* plants. Fluorescence was observed with a confocal laser scanning microscope (Axio imager Z2; Zeiss).

In Vitro Phosphorylation Assay

To identify the phosphorylation sites in IIP4, we incubated the purified recombinant His-tagged IIP4 and GST-tagged ILA1 together as described previously (Ning et al., 2011). The resultant products were separated on SDS-PAGE gel and then stained with Coomassie brilliant blue. The gel containing IIP4 was sliced. After digestion by trypsin, the samples were subjected to a Linear ion trap mass spectrometer (Thermo Finnigan) for mass spectrometry analysis. The phosphorylated peptides were analyzed using Bioworks software (Thermo). This analysis was conducted three times.

Bioinformatics Analyses

Alignment of IIP4 and its homologs in rice and other species was conducted using ClustalX (Larkin et al., 2007) based on the sequences from rice genome database (<http://rice.plantbiology.msu.edu>) and NCBI (<http://www.ncbi.nlm.nih.gov/>), and analyzed with Jalview (Waterhouse et al., 2009). Sequence logos of CCCH motifs in each protein were generated online with the application of WebLogo3 (Crooks et al., 2004). The IIP4 homologs were identified in the species based on known sequences from the PLAZA 2.5 database (<http://bioinformatics.psb.ugent.be/plaza>). A phylogenetic tree of IIP4 homologs from representative plant species was built using neighbor joining in MEGA6 software (Tamura et al., 2013). One thousand bootstrap replicates were performed to infer bootstrap values shown next to the branches as percentage.

SUPPLEMENTAL INFORMATION

Supplemental Information is available at *Molecular Plant Online*.

FUNDING

This research was supported by the National Nature Science Foundation of China (31530051 and 31370310), CAS grants for XDA08010103, Youth Innovation Promotion Association CAS (2016094), and the Ministry of Agriculture of China (2016ZX08009-003), as well as the State Key Laboratory of Plant Genomics.

AUTHOR CONTRIBUTIONS

Y.Z. and B.Z. conceived the study; D.Z. conducted the major analyses in this work; Z.X. and X.L. performed gene transformation and field work; S.C. and S.L. performed gene expression and cell wall composition analyses; K.C. and C.G. designed and prepared the construct for the CRISPR/Cas9 assay; Y.Z. and B.Z. wrote the article.

ACKNOWLEDGMENTS

We thank Prof. Weicai Yang, Institute of Genetics and Developmental Biology, Chinese Academy of Sciences (IGDB, CAS) for help with laser microdissection, and Lijun Zhang from IGDB, CAS for help with lignin analysis. No conflict of interest declared.

Received: June 29, 2017

Revised: November 9, 2017

Accepted: November 13, 2017

Published: November 21, 2017

REFERENCES

- Bhargava, A., Ahad, A., Wang, S., Mansfield, S.D., Haughn, G.W., Douglas, C.J., and Ellis, B.E. (2013). The interacting MYB75 and KNAT7 transcription factors modulate secondary cell wall deposition both in stems and seed coat in *Arabidopsis*. *Planta* **237**:1199–1211.
- Brutus, A., Sicilia, F., Macone, A., Cervone, F., and De Lorenzo, G. (2010). A domain swap approach reveals a role of the plant wall-associated kinase 1 (WAK1) as a receptor of oligogalacturonides. *Proc. Natl. Acad. Sci. USA* **107**:9452–9457.
- Carlsbecker, A., Lee, J.Y., Roberts, C.J., Dettmer, J., Lehesranta, S., Zhou, J., Lindgren, O., Moreno-Risueno, M.A., Vaten, A., Thitamadee, S., et al. (2010). Cell signalling by microRNA165/6 directs gene dose-dependent root cell fate. *Nature* **465**:316–321.
- Chai, G., Qi, G., Cao, Y., Wang, Z., Yu, L., Tang, X., Yu, Y., Wang, D., Kong, Y., and Zhou, G. (2014). Poplar PdC3H17 and PdC3H18 are direct targets of PdMYB3 and PdMYB21, and positively regulate secondary wall formation in *Arabidopsis* and poplar. *New Phytol.* **203**:520–534.
- Ciftci-Yilmaz, S., and Mittler, R. (2008). The zinc finger network of plants. *Cell Mol. Life Sci.* **65**:1150–1160.
- Crooks, G.E., Hon, G., Chandonia, J.M., and Brenner, S.E. (2004). WebLogo: a sequence logo generator. *Genome Res.* **14**:1188–1190.
- Dubos, C., Stracke, R., Grotewold, E., Weisshaar, B., Martin, C., and Lepiniec, L. (2010). MYB transcription factors in *Arabidopsis*. *Trends Plant Sci.* **15**:573–581.

- Fornale, S., Shi, X., Chai, C., Encina, A., Irar, S., Capellades, M., Fuguet, E., Torres, J.L., Rovira, P., Puigdomenech, P., et al. (2010). ZmMYB31 directly represses maize lignin genes and redirects the phenylpropanoid metabolic flux. *Plant J.* **64**:633–644.
- Gao, Y., He, C., Zhang, D., Liu, X., Xu, Z., Tian, Y., Liu, X.H., Zang, S., Pauly, M., Zhou, Y., et al. (2017). Two trichome birefringence-like proteins mediate xylan acetylation, which is essential for leaf blight resistance in rice. *Plant Physiol.* **173**:470–481.
- Handakumbura, P.P., and Hazen, S.P. (2012). Transcriptional regulation of grass secondary cell wall biosynthesis: playing catch-up with *Arabidopsis thaliana*. *Front. Plant Sci.* **3**:74.
- Hiratsu, K., Matsui, K., Koyama, T., and Ohme-Takagi, M. (2003). Dominant repression of target genes by chimeric repressors that include the EAR motif, a repression domain, in *Arabidopsis*. *Plant J.* **34**:733–739.
- Hu, K., Cao, J., Zhang, J., Xia, F., Ke, Y., Zhang, H., Xie, W., Liu, H., Cui, Y., Cao, Y., et al. (2017). Improvement of multiple agronomic traits by a disease resistance gene via cell wall reinforcement. *Nat. Plants* **3**:17009.
- Huang, D., Wang, S., Zhang, B., Shang-Guan, K., Shi, Y., Zhang, D., Liu, X., Wu, K., Xu, Z., Fu, X., et al. (2015). A gibberellin-mediated DELLA-NAC signaling cascade regulates cellulose synthesis in rice. *Plant Cell* **27**:1681–1696.
- Jan, A., Maruyama, K., Todaka, D., Kidokoro, S., Abo, M., Yoshimura, E., Shinozaki, K., Nakashima, K., and Yamaguchi-Shinozaki, K. (2013). OsTZF1, a CCCH-tandem zinc finger protein, confers delayed senescence and stress tolerance in rice by regulating stress-related genes. *Plant Physiol.* **161**:1202–1216.
- Jin, H., Cominelli, E., Bailey, P., Parr, A., Mehrtens, F., Jones, J., Tonelli, C., Weisshaar, B., and Martin, C. (2000). Transcriptional repression by AtMYB4 controls production of UV-protecting sunscreens in *Arabidopsis*. *EMBO J.* **19**:6150–6161.
- Kim, W.C., Ko, J.H., and Han, K.H. (2012). Identification of a cis-acting regulatory motif recognized by MYB46, a master transcriptional regulator of secondary wall biosynthesis. *Plant Mol. Biol.* **78**:489–501.
- Ko, J.H., Kim, W.C., and Han, K.H. (2009). Ectopic expression of MYB46 identifies transcriptional regulatory genes involved in secondary wall biosynthesis in *Arabidopsis*. *Plant J.* **60**:649–665.
- Kubo, M., Udagawa, M., Nishikubo, N., Horiguchi, G., Yamaguchi, M., Ito, J., Mimura, T., Fukuda, H., and Demura, T. (2005). Transcription switches for protoxylem and metaxylem vessel formation. *Gene Dev.* **19**:1855–1860.
- Larkin, M.A., Blackshields, G., Brown, N.P., Chenna, R., McGettigan, P.A., McWilliam, H., Valentin, F., Wallace, I.M., Wilm, A., Lopez, R., et al. (2007). Clustal W and clustal X version 2.0. *Bioinformatics* **23**:2947–2948.
- Legay, S., Sivadon, P., Blervacq, A.S., Pavy, N., Baghdady, A., Tremblay, L., Levasseur, C., Ladouce, N., Lapierre, C., Seguin, A., et al. (2010). EgMYB1, an R2R3 MYB transcription factor from eucalyptus negatively regulates secondary cell wall formation in *Arabidopsis* and poplar. *New Phytol.* **188**:774–786.
- Leivar, P., and Quail, P.H. (2011). PIFs: pivotal components in a cellular signaling hub. *Trends Plant Sci.* **16**:19–28.
- Li, E., Bhargava, A., Qiang, W., Friedmann, M.C., Forneris, N., Savidge, R.A., Johnson, L.A., Mansfield, S.D., Ellis, B.E., and Douglas, C.J. (2012a). The Class II KNOX gene *KNAT7* negatively regulates secondary wall formation in *Arabidopsis* and is functionally conserved in *Populus*. *New Phytol.* **194**:102–115.
- Li, E., Wang, S., Liu, Y., Chen, J.G., and Douglas, C.J. (2011). OVATE FAMILY PROTEIN4 (OFP4) interaction with *KNAT7* regulates secondary cell wall formation in *Arabidopsis thaliana*. *Plant J.* **67**:328–341.
- Li, Q., Lin, Y.C., Sun, Y.H., Song, J., Chen, H., Zhang, X.H., Sederoff, R.R., and Chiang, V.L. (2012b). Splice variant of the SND1 transcription factor is a dominant negative of SND1 members and their regulation in *Populus trichocarpa*. *Proc. Natl. Acad. Sci. USA* **109**:14699–14704.
- Li, Z., and Thomas, T.L. (1998). *PEI1*, an embryo-specific zinc finger protein gene required for heart-stage embryo formation in *Arabidopsis*. *Plant Cell* **10**:383–398.
- McCarthy, R.L., Zhong, R., and Ye, Z.H. (2009). MYB83 is a direct target of SND1 and acts redundantly with MYB46 in the regulation of secondary cell wall biosynthesis in *Arabidopsis*. *Plant Cell Physiol.* **50**:1950–1964.
- Mitsuda, N., and Ohme-Takagi, M. (2008). NAC transcription factors NST1 and NST3 regulate pod shattering in a partially redundant manner by promoting secondary wall formation after the establishment of tissue identity. *Plant J.* **56**:768–778.
- Mitsuda, N., Seki, M., Shinozaki, K., and Ohme-Takagi, M. (2005). The NAC transcription factors NST1 and NST2 of *Arabidopsis* regulate secondary wall thickenings and are required for anther dehiscence. *Plant Cell* **17**:2993–3006.
- Ning, J., Zhang, B., Wang, N., Zhou, Y., and Xiong, L. (2011). Increased leaf angle1, a Raf-like MAPKKK that interacts with a nuclear protein family, regulates mechanical tissue formation in the lamina joint of rice. *Plant Cell* **23**:4334–4347.
- Schumann, U., Prestele, J., O’Geen, H., Brueggeman, R., Wanner, G., and Gietl, C. (2007). Requirement of the C3HC4 zinc RING finger of the *Arabidopsis* PEX10 for photorespiration and leaf peroxisome contact with chloroplasts. *Proc. Natl. Acad. Sci. USA* **104**:1069–1074.
- Shan, Q., Wang, Y., Li, J., Zhang, Y., Chen, K., Liang, Z., Zhang, K., Liu, J., Xi, J.J., Qiu, J.L., et al. (2013). Targeted genome modification of crop plants using a CRISPR-Cas system. *Nat. Biotechnol.* **31**:686–688.
- Tamura, K., Stecher, G., Peterson, D., Filipski, A., and Kumar, S. (2013). MEGA6: molecular evolutionary genetics analysis version 6.0. *Mol. Biol. Evol.* **30**:2725–2729.
- Taylor-Teeples, M., Lin, L., de Lucas, M., Turco, G., Toal, T.W., Gaudinier, A., Young, N.F., Trabucco, G.M., Veling, M.T., Lamothe, R., et al. (2015). An *Arabidopsis* gene regulatory network for secondary cell wall synthesis. *Nature* **517**:571–575.
- Updegraff, D.M. (1969). Semimicro determination of cellulose in biological materials. *Anal. Biochem.* **32**:420–424.
- Wang, H., Avci, U., Jin, N., Hahn, M.G., Chen, F., and Dixon, R.A. (2010). Mutation of WRKY transcription factors initiates pith secondary wall formation and increases stem biomass in dicotyledonous plants. *Proc. Natl. Acad. Sci. USA* **107**:22338–22343.
- Watanabe, Y., Meents, M.J., McDonnell, L.M., Barkwill, S., Sampathkumar, A., Cartwright, H.N., Demura, T., Ehrhardt, D.W., Samuels, A.L., and Mansfield, S.D. (2015). Visualization of cellulose synthases in *Arabidopsis* secondary cell walls. *Science* **350**:198–203.
- Waterhouse, A.M., Procter, J.B., Martin, D.M., Clamp, M., and Barton, G.J. (2009). Jalview Version 2—a multiple sequence alignment editor and analysis workbench. *Bioinformatics* **25**:1189–1191.
- Xie, L., Yang, C., and Wang, X. (2011). Brassinosteroids can regulate cellulose biosynthesis by controlling the expression of *CESA* genes in *Arabidopsis*. *J. Exp. Bot.* **62**:4495–4506.
- Xiong, G., Li, R., Qian, Q., Song, X., Liu, X., Yu, Y., Zeng, D., Wan, J., Li, J., and Zhou, Y. (2010). The rice dynamin-related protein DRP2B mediates membrane trafficking, and thereby plays a critical role in secondary cell wall cellulose biosynthesis. *Plant J.* **64**:56–70.
- Xu, B., Ohtani, M., Yamaguchi, M., Toyooka, K., Wakazaki, M., Sato, M., Kubo, M., Nakano, Y., Sano, R., Hiwatashi, Y., et al. (2014). Contribution of NAC transcription factors to plant adaptation to land. *Science* **343**:1505–1508.

Molecular Plant

- Xu, S.L., Rahman, A., Baskin, T.I., and Kieber, J.J.** (2008). Two leucine-rich repeat receptor kinases mediate signaling, linking cell wall biosynthesis and ACC synthase in *Arabidopsis*. *Plant Cell* **20**:3065–3079.
- Yamaguchi, M., Kubo, M., Fukuda, H., and Demura, T.** (2008). Vascular-related NAC-DOMAIN7 is involved in the differentiation of all types of xylem vessels in *Arabidopsis* roots and shoots. *Plant J.* **55**:652–664.
- Yamaguchi, M., Ohtani, M., Mitsuda, N., Kubo, M., Ohme-Takagi, M., Fukuda, H., and Demura, T.** (2010). VND-INTERACTING2, a NAC domain transcription factor, negatively regulates xylem vessel formation in *Arabidopsis*. *Plant Cell* **22**:1249–1263.
- Zhang, B., Zhang, L., Li, F., Zhang, D., Liu, X., Wang, H., Xu, Z., Chu, C., and Zhou, Y.** (2017). Control of secondary cell wall patterning involves xylan deacetylation by a GDSL esterase. *Nat. Plants* **3**:17017.
- Zhao, Y., Sun, J., Xu, P., Zhang, R., and Li, L.** (2014). Intron-mediated alternative splicing of WOOD-ASSOCIATED NAC TRANSCRIPTION

A Repressor of Secondary Wall Synthesis

- FACTOR1B regulates cell wall thickening during fiber development in *Populus* species. *Plant Physiol.* **164**:765–776.
- Zhong, R., Lee, C., Zhou, J., McCarthy, R.L., and Ye, Z.H.** (2008). A battery of transcription factors involved in the regulation of secondary cell wall biosynthesis in *Arabidopsis*. *Plant Cell* **20**:2763–2782.
- Zhong, R., Richardson, E.A., and Ye, Z.H.** (2007). Two NAC domain transcription factors, SND1 and NST1, function redundantly in regulation of secondary wall synthesis in fibers of *Arabidopsis*. *Planta* **225**:1603–1611.
- Zhong, R., and Ye, Z.H.** (2007). Regulation of cell wall biosynthesis. *Curr. Opin. Plant Biol.* **10**:564–572.
- Zhong, R., and Ye, Z.H.** (2014). Complexity of the transcriptional network controlling secondary wall biosynthesis. *Plant Sci.* **229**:193–207.